Synthesis, Coordination Behavior, and Use in Asymmetric Hydrogenations of Walphos-Type Ligands

Yaping Wang,[†] Thomas Sturm,[†,¶] Marianne Steurer,[†] Vladimir B. Arion,[‡,△] Kurt Mereiter,[§,△] Felix Spindler,*[,⊥] and Walter Weissensteiner*[,†]

Institute of Organic Chemistry, University of Vienna, Währinger Strasse 38, A-1090 Vienna, Austria, Institute of Inorganic Chemistry, University of Vienna, Währinger Strasse 42, A-1090 Vienna, Austria, Institute of Chemical Technologies and Analytics, Vienna University of Technology, Getreidemarkt 9/164SC, A-1060 Vienna, Austria, and Solvias AG, Catalysis Research, P.O. Box, CH-4002 Basel, Switzerland

Received November 1, 2007

A total of nine Walphos-type diphosphine ligands, all of which have a ferrocenyl-aryl backbone, have been synthesized, characterized, and tested in asymmetric ruthenium-, rhodium-, and iridium-catalyzed hydrogenations of alkenes, ketones, and one imine. Ruthenium- and rhodium-mediated hydrogenations of alkenes and ketones gave enantioselectivities of up to 95% and 97% ee, respectively. Ligand tuning was attempted by variation of the phosphorus-bound aryl and alkyl substituents and by attaching electron-donating or electron-withdrawing substituents to the backbone phenyl ring. Dichloropalladium(II) complexes of five ligands were synthesized, and in four cases the molecular structures were studied in solution as well as in the solid state.

Introduction

Ferrocene-based diphosphines constitute a well-established class of ligands for transition metals that have a broad range of applications in asymmetric catalysis.[1] In a previous communication we briefly reported on a class of ferrocenyl-aryl-based diphosphine ligands, which we named the Walphos ligand family (**1a**–**1e**, Chart 1).[2] The use of these ligands in rhodium- and ruthenium-catalyzed asymmetric hydrogenations of olefins and ketones gave enantioselectivities of up to 95% and 97% ee, respectively. Furthermore, one Walphos-type ligand (**1c**) proved to be highly suitable for the asymmetric hydrogenation of a 2-isopropylcinnamic acid derivative, an intermediate in the industrial synthesis of the renin inhibitor aliskiren.[3] In addition to hydrogenations,[2,4] including cluster-based hydrogenations,[5] Walphos-type ligands were successfully applied in a number of other catalytic reactions such as nitroso-Diels–Alder reactions,[6] reductive coupling reactions of enynes and ketoesters,[7] [4 + 2] carbocyclizations,[8] conjugate reductions of acyclic enones,[9] diastereoselective Hartwig–Buchwald reactions,[10] and others.[11]

Chart 1

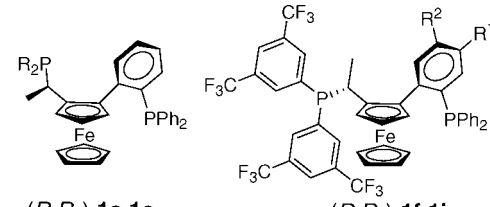

(R,R_p)-**1a-1e**

	R =
a	Cy
b	*tert*-Bu
c	[3,5-$(CF_3)_2$-C_6H_3]
d	Ph
e	[3,5-Me_2-4-OMe-C_6H_2]

(R,R_p)-**1f-1i**

	R^1 =	R^2 =
f	CF_3	H
g	CH_3	H
h	OCH_3	H
i	OCH_3	OCH_3

As one would expect, tuning of the steric and electronic properties of catalyst ligands to the respective reactions and

* Corresponding author. E-mail: walter.weissenstreiner@univie.ac.at.
† University of Vienna, Institute of Organic Chemistry.
‡ University of Vienna, Institute of Inorganic Chemistry.
§ Vienna University of Technology.
⊥ Solvias AG.
¶ Present address: Donau Chemie AG, A-3435 Pischelsdorf, Austria.
△ Crystallography.

(1) (a) Blaser, H. U.; Pugin, B.; Spindler, F.; Thommen, M. *Acc. Chem. Res.* **2007**, *40*, 1240−1250. (b) Whittall, J. Industrial Catalysts for Regio- or Stereo-Selective Oxidations and Reductions. A Review of Key Technologies and Targets. In *Catalysts for Fine Chemical Synthesis, Vol. 5, Regio- and Stereo-Controlled Oxidations and Reductions*; Roberts, S., Whittall, J., Eds.; Wiley: Weinheim, 2007; pp 2–34. (c) Gomez Arrayás, R.; Adrio, J.; Carretero, J. C. *Angew. Chem., Int. Ed.* **2006**, *45*, 7674–7715. (d) Barbaro, P.; Bianchini, C.; Giambastiani, G.; Parisel, S. L. *Coord. Chem. Rev.* **2004**, *248*, 2131–2150. (e) Atkinson, R. C. J.; Gibson, V. C.; Long, N. J. *Chem. Soc. Rev.* **2004**, *33*, 313–328. (f) Blaser, H. U., Schmidt, E., Eds. *Asymmetric Catalysis on Industrial Scale: Challenges, Approaches and Solutions*; Wiley-VCH: Weinheim, 2004. (g) Colacot, T. J. *Chem. Rev.* **2003**, *103*, 3101–3118. (h) Ojima, I., Ed. *Catalytic Asymmetric Synthesis*; Wiley-VCH: New York, 2000.

(2) Sturm, T.; Weissensteiner, W.; Spindler, F. *Adv. Synth. Catal.* **2003**, *345*, 160–164.

(3) Stutz, S.; Herold, P.; Spindler, F.; Weissensteiner, W.; Sturm, T. U.S. Patent Appl. US 2003139625, 2003 (PCT Int. Appl. WO 0202500, Solvias A.-G., Switz., 2002).

(4) (a) Herold, P.; Stutz, S.; Mah, R.; Stojanovic, A.; Lyothier, I.; Behnke, D.; Spindler, F.; Bappert, E. PCT Int. Appl. WO 2007085651, 2007. (b) Moran, W. J.; Morken, J. P. *Org. Lett.* **2006**, *8*, 2413–2415. (c) Stephenson, P.; Kondor, B.; Licence, P.; Scovell, K.; Ross, S. K.; Poliakoff, M. *Adv. Synth. Catal.* **2006**, *348*, 1605–1610. (d) Houpis, I. N.; Patterson, L. E.; Alt, C. A.; Rizzo, J. R.; Zhang, T. Y.; Haurez, M. *Org. Lett.* **2005**, *7*, 1947–1950. (e) Pugin, B.; Studer, M.; Kuesters, E.; Sedelmeier, G.; Feng, X. *Adv. Synth. Catal.* **2004**, *346*, 1481–1486. (f) Morgan, J. B.; Morken, J. P. *J. Am. Chem. Soc.* **2004**, *126*, 15338–15339. (g) Bänziger, M.; Cercus, J.; Hirt, H.; Laumen, K.; Malan, C.; Spindler, F.; Struber, F.; Troxler, T. *Tetrahedron: Asymmetry* **2003**, *14*, 3469–3477.

(5) Moberg, V.; Haukka, M.; Koshevoy, I. O.; Ortiz, R.; Nordlander, E. *Organometallics* **2007**, *26*, 4090–4093.

(6) Jana, C. K.; Studer, A. *Angew. Chem., Int. Ed.* **2007**, *46*, 6542–6544.

(7) (a) Komanduri, V.; Krische, M. J. *J. Am. Chem. Soc.* **2006**, *128*, 16448–16449. (b) Kong, J.-R.; Ngai, M.-Y.; Krische, M. J. *J. Am. Chem. Soc.* **2006**, *128*, 718–719.

10.1021/om701103d CCC: $40.75
Publication on Web 02/19/2008

substrates is a requirement for optimal catalyst performance. To date, Walphos-type ligands have only been tuned by varying the steric and electronic properties of the phosphorus-linked substituents. Therefore, we questioned whether additional fine-tuning, particularly fine-tuning of the electronic properties of ligands and their metal complexes, could be achieved by attaching electron-withdrawing or electron-donating substituents to the ligand backbone at positions remote from the phosphino groups.

For this purpose we synthesized four novel analogues of the industrially important ligand **1c** by attaching electron-withdrawing (CF_3) or electron-donating (CH_3, OCH_3) groups to position 4 (**1f**–**1h**) and, in one case (**1i**), to positions 4 and 5 of the phenyl ring directly linked to the ferrocenyl Cp-ring.

In order to study the coordination behavior of such diphosphines, dichloropalladium(II) complexes of several representative ligands were prepared as model compounds, and the molecular structures of four complexes were determined by X-ray diffraction. All newly synthesized ligands were tested in asymmetric hydrogenation reactions of alkenes, ketones, and one imine, and the results obtained were compared to those reported previously for ligands **1a**–**1e**.

Results and Discussion

Synthesis of Diphosphines 1f–1i and Dichloropalladium(II) Complexes of Ligands (*R*,*R*$_p$)-1c, (*R*,*R*$_p$)-1d, (*S*,*R*$_p$)-1d, (*R*,*R*$_p$)-1f, and (*R*,*R*$_p$)-1i. As for the parent ligands **1a**–**1e** (for details see Supporting Information), the synthesis of **1f**–**1i** started from enantiomerically pure amine (*R*)-**2**[12] (Scheme 1), which in the first step was *ortho*-lithiated with *sec*-butyllithium and further reacted with $ZnCl_2$. A subsequent palladium-mediated Negishi-type coupling[13] with the appropriate 2-bromo-1-iodobenzene derivatives gave the intermediates (*R*,*R*$_p$)-**3f**–**3i**. Yields in the Negishi coupling reactions strongly depended on the electronic properties of the aryl iodides used. For example, the electron-poor 2-bromo-4-trifluoromethyliodobenzene gave only 27% yield of product, while use of the electron-rich 2-bromo-4,5-dimethoxyiodobenzene led to a yield of 45%. In the next step the coupling products **3f**–**3i** were reacted with *sec*-BuLi (THF/–40 °C). Subsequent quenching with chlorodiphenylphosphine oxide at room temperature resulted in the aminophosphine oxides (*R*,*R*$_p$)-**4f**–**4i** (yields

Scheme 1. Synthesis of Walphos-Type ligands 1f–1i

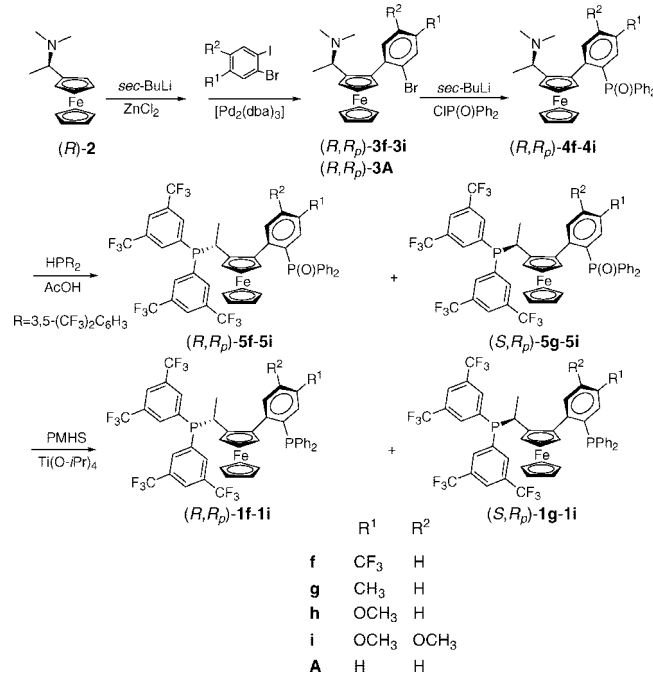

>90%). On heating mixtures of phosphine oxides **4f**–**4i** and bis[3,5-di(trifluoromethyl)phenyl]phosphine in acetic acid[14] for several hours at 100 °C, the dimethylamino group was replaced in all cases in a nucleophilic substitution reaction by a diarylphosphino unit and phosphine-phosphine oxides **5f**–**5i** were obtained in about 80% yield. Only in the case of **4f** (R^1 = CF_3, R^2 = H) was a single diastereomer (**5f**) obtained, and this had the expected (*R*,*R*$_p$) absolute configuration, indicating clean retention of configuration at the stereogenic center. In all other cases a mixture of diastereomers, (*R*,*R*$_p$)-**5g**–**5i** and (*S*,*R*$_p$)-**5g**–**5i** in a ratio of about 10:1 (determined by ^{31}P NMR spectroscopy), was isolated and separated by chromatography. It is interesting to note that in this particular step of the original syntheses of ligands **1a**–**1e** the corresponding intermediates **5a**, **5b**, and **5e** were obtained as single isomers, while **5c** and **5d** were formed as mixtures of diastereomers in ratios of 10:1 and 6:1, respectively. It is clear that this reaction step depends on the nucleophilicity of the dialkyl- or diarylphosphine used, since only electron-rich phosphines gave products with full retention of configuration at the stereogenic center. The configurational assignment of diastereomers was confirmed by an X-ray diffraction study on the dichloropalladium(II) complexes of ligands (*R*,*R*$_p$)-**1d** and (*S*,*R*$_p$)-**1d** (see below). In the final step all of the phosphine-phosphine oxides **5f**–**5i** were reduced to the respective diphosphine ligands **1f**–**1i**. In addition to polymethylhydrosiloxane/titanium isopropoxide, which we had used previously, trimethylsilyl trifluoromethanesulfonate (TMSOTf)/$LiAlH_4$ was also tested as the reducing agent.[15] However, the latter reducing agent led to the formation of slightly larger amounts of byproduct. Dichloropalladium(II) complexes of ligands (*R*,*R*$_p$)-**1c**, (*R*,*R*$_p$)-**1d**, (*S*,*R*$_p$)-**1d**, (*R*,*R*$_p$)-**1f**, and (*R*,*R*$_p$)-**1i** were prepared by reacting the appropriate diphosphines with dichlorobis(acetonitrile)palladium(II).

The structural integrity of all compounds, i.e., (*R*,*R*$_p$)-**1a**–**1i**, (*S*,*R*$_p$)-**1d**, (*S*,*R*$_p$)-**1g**, and dichloropalladium(II) complexes

(8) (a) Tanaka, K.; Hagiwara, Y.; Hirano, M. *Eur. J. Org. Chem.* **2006**, 3582–3595. (b) Tanaka, K.; Hagiwara, Y.; Noguchi, K. *Angew. Chem., Int. Ed. Engl.* **2005**, *44*, 7260–7263.

(9) (a) Lipshutz, B. H.; Noson, K.; Chrisman, W.; Lower, A. *J. Am. Chem. Soc.* **2003**, *125*, 8779–8789. (b) Lipshutz, B. H.; Servesko, J. M. *Angew. Chem., Int. Ed.* **2003**, *42*, 4789–4792.

(10) Kreis, M.; Friedmann, C. J.; Braese, S. *Chem.−Eur. J.* **2005**, *11*, 7387–7394.

(11) (a) Umeda, R.; Studer, A. *Org. Lett.* **2007**, *9*, 2175–2178. (b) Stemmler, R. T.; Bolm, C. *Adv. Synth. Catal.* **2007**, *349*, 1185–1198. (c) Chuzel, O.; Deschamp, J.; Chausteur, C.; Riant, O. *Org. Lett.* **2006**, *8*, 5943–5946. (d) Godard, C.; Ruiz, A.; Claver, C. *Helv. Chim. Acta* **2006**, *89*, 1610–1622. (e) Axtell, A. T.; Klosin, J.; Abboud, K. A. *Organometallics* **2006**, *25*, 5003–5009. (f) Cho, C-W.; Krische, M. J. *Org. Lett.* **2006**, *8*, 3873–3876. (g) Llamas, T.; Arrayás, R. G.; Carretero, J. C. *Org. Lett.* **2006**, *8*, 1795–1798. (h) Phua, P. H.; White, A. J. P.; de Vries, J. G.; Hii, K. K. *Adv. Synth. Catal.* **2006**, *348*, 587–592. (i) Deschamp, J.; Chuzel, O.; Hannedouche, J.; Riant, O. *Angew. Chem., Int. Ed.* **2006**, *45*, 1292–1297. (j) Lipshutz, B. H.; Frieman, B. A.; Unger, J. B.; Nihan, D. M. *Can. J. Chem.* **2005**, *83*, 606–614. (k) Munoz, M. P.; Adrio, J.; Carretero, J. C.; Echavarren, A. M. *Organometallics* **2005**, *24*, 1293–1300. (l) Berkowitz, D. B.; Maiti, G. *Org. Lett.* **2004**, *6*, 2661–2664. (m) Markert, C.; Pfaltz, A. *Angew. Chem., Int. Ed.* **2004**, *43*, 2498–2500.

(12) Marquarding, D.; Klusacek, H.; Gokel, G.; Hoffmann, P.; Ugi, I. *J. Am. Chem. Soc.* **1970**, *92*, 5389–5393.

(13) Negishi, E.; Liu, F. In *Metal-catalyzed Cross-coupling Reactions*; Diederich, F., Stang, P. J., Eds.; Wiley-VCH: Weinheim, 1998; pp 1–47..

(14) Togni, A.; Breutel, C.; Schnyder, A.; Spindler, F.; Landert, H.; Tijani, A. *J. Am. Chem. Soc.* **1994**, *116*, 4062–4066.

(15) Imamoto, T.; Kikuchi, S.; Miura, T.; Wada, Y. *Org. Lett.* **2001**, *3*, 87–90.

Table 1. Details for the Crystal Structure Determinations of Complexes [$PdCl_2$(L)], L = (*R*,*R*$_p$)-1d, (*S*,*R*$_p$)-1d, (*R*,*R*$_p$)-1f, (*R*,*R*$_p$)-1i

	[$PdCl_2$((*R*,*R*$_p$)-**1d**)]	[$PdCl_2$((*S*,*R*$_p$)-**1d**)]	[$PdCl_2$((*R*,*R*$_p$)-**1f**)]	[$PdCl_2$((*R*,*R*$_p$)-**1i**)]
formula	$C_{42}H_{36}Cl_2FeP_2Pd.CHCl_3$	$C_{42}H_{36}Cl_2FeP_2Pd.CHCl_3$	$2(C_{47}H_{31}C_{12}F_{15}FeP_2Pd)\ .CHCl_3$	$C_{48}H_{36}Cl_2F_{12}FeO_2P_2Pd\ 0.3(CHCl_3)$
fw	955.17	955.17	2471.03	1525.96
cryst size, mm	0.58 × 0.34 × 0.28	0.48 × 0.32 × 0.20	0.26 × 0.20 × 0.08	0.32 × 0.20 × 0.14
space group	$P2_1$ (no. 4)	$P2_1$ (no. 4)	$P2_12_12_1$ (no. 19)	$P2_12_12_1$ (no. 19)
a, Å	11.278(2)	11.566(3)	12.3737(4)	10.4499(4)
b, Å	14.443(3)	11.258(3)	26.4570(7)	23.0779(11)
c, Å	13.142(3)	15.813(5)	29.0299(10)	24.5543(11)
β, deg	102.80(1)	98.68(1)		
V, Å^3	2087.5(7)	2035.4(10)	9503.5(5)	5921.6(4)
Z	2	2	4	4
ρ_{calc}, g cm^{-3}	1.520	1.558	1.727	1.712
T, K	297	297	100	100
μ, mm^{-1} (Mo Kα)	1.205	1.236	1.042	1.177
F(000)	964	964	4904	3032
θ_{max}, deg	30.0	30.0	28.35	29.46
no. of rflns measd	38 247	29 849	255 912	132 701
no. of unique rflns	12 031	11 591	23 656	16 331
no. of rflns I > 2σ(I)	11 502	10 970	20 782	14 587
no. of params	481	470	1261	732
R_1 ($I > 2\sigma(I)$)[a]	0.0237	0.0212	0.0418	0.0363
R_1 (all data)	0.0255	0.0229	0.0537	0.0451
wR_2 (all data)	0.0626	0.0521	0.1012	0.0808
Flack abs str param	−0.017(10)	−0.015(9)	−0.004(12)	−0.008(12)
diff Fourier peaks min./max., e Å^{-3}	−0.55/0.55	−0.57/0.45	−1.22/1.26	−0.59/0.92

[a] $R_1 = \sum||F_o| - |F_c||/\sum|F_o|$, $wR_2 = [\sum(w(F_o^2 - F_c^2)^2)/\sum(w(F_o^2)^2)]^{1/2}$.

[$PdCl_2$(L)], L = (*R*,*R*$_p$)-**1c**, (*R*,*R*$_p$)-**1d**, (*S*,*R*$_p$)-**1d**, (*R*,*R*$_p$)-**1f**, and (*R*,*R*$_p$)-**1i**, was assessed by NMR spectroscopy, and in four cases, single crystals were also studied by X-ray diffraction (see below). The ^{31}P NMR spectra of diphosphines **1a**–**1i** show some interesting features. For ligands (*R*,*R*$_p$)-**1a**–**1i**, the signals of the PPh_2 phosphorus directly attached to the backbone aryl ring all lie within a very narrow range of chemical shifts (δ = –13.2 to –14.5 ppm). For all ligands of (*R*,*R*$_p$) configuration bearing a diarylphosphino unit at the ferrocenylethyl side chain [(*R*,*R*$_p$)-**1c**–**1i**], the Ar_2P-phosphorus signals appear between δ = 2.2 and 4.0 ppm. Interestingly, the phosphorus signals for ligands with the (*S*,*R*$_p$)-configuration are always shifted to higher field than those of their corresponding diastereomers with the (*R*,*R*$_p$)-configuration [high-field shift for ligands (*S*,*R*$_p$)-**1c**, (*S*,*R*$_p$)-**1d**, and (*S*,*R*$_p$)-**1g**–**1i** versus (*R*,*R*$_p$)-**1c**, (*R*,*R*$_p$)-**1d**, and (*R*,*R*$_p$)-**1g**–**1i**; Ar_2P: 5.6–8.8 ppm, Ph_2P: 0.7–1.3 ppm].

The absolute (*R*$_p$)-configuration of ligands **1a**–**1i** follows from the known absolute configuration of the starting material (*R*)-**2** and the known direction and diastereoselectivity of its *ortho*-lithiation with *sec*-BuLi that, after a Negishi-type coupling, led to intermediates (*R*,*R*$_p$)-**3**. An X-ray diffraction study of the ammonium iodide salt of (*R*,*R*$_p$)-**3A** [(*R*,*R*$_p$)-**3A**.HI] (**3A**: precursor of ligands **1a**–**1e**, $R^1 = R^2$ = H, Scheme 1) proved this assignment (for details see Supporting Information). Furthermore, X-ray diffraction on complexes [$PdCl_2$(L)], L = (*R*,*R*$_p$)-**1d**, (*S*,*R*$_p$)-**1d**, (*R*,*R*$_p$)-**1f**, (*R*,*R*$_p$)-**1i**, also confirmed the absolute (*R*$_p$)-configuration at ferrocene as well as the assignment of the relative configurations of the respective stereogenic centers.

Molecular Structures of Complexes [$PdCl_2$(L)], L = (*R*,*R*$_p$)-1c, (*R*,*R*$_p$)-1d, (*S*,*R*$_p$)-1d, (*R*,*R*$_p$)-1f, and (*R*,*R*$_p$)-1i. As mentioned above, diphosphines **1c**, **1d**, and **1g**–**1i** were obtained in two diastereomeric forms. In order to assign their relative configurations and to study the coordination behavior of such diphosphines, dichloropalladium(II) complexes [$PdCl_2$(L)] of ligands (*R*,*R*$_p$)-**1d** and (*S*,*R*$_p$)-**1d** were prepared as model compounds and their structures were determined in the solid state. In addition, we questioned how the influence of electron-withdrawing or electron-donating substituents in the ligand backbone (e.g., ligands **1f** and **1i**) would be reflected in their respective metal complexes. Therefore, dichloropalladium(II) complexes [$PdCl_2$(L)] of ligands (*R*,*R*$_p$)-**1c**, (*R*,*R*$_p$)-**1f**, and (*R*,*R*$_p$)-**1i** were also prepared.

The molecular structures of complexes [$PdCl_2$(L)] [L = (*R*,*R*$_p$)-**1d**, (*S*,*R*$_p$)-**1d**, (*R*,*R*$_p$)-**1f**, and (*R*,*R*$_p$)-**1i**] in the solid state were determined by X-ray diffraction.[16] In all cases single crystals were obtained by diffusion of diethyl ether into a solution of the respective complex in $CHCl_3$. Details on X-ray crystallography experiments are given in Table 1 and in the Experimental Section. Views of the molecular structures of these compounds are shown in Figure 1, and selected geometrical data are given in Table 2. The absolute configuration of each compound was determined from the X-ray anomalous dispersion effects and was consistent with the chemical evidence.

The molecular structures of complexes [$PdCl_2$(**1d**)] proved both the relative and the absolute configuration of ligand **1d** to be (*R*,*R*$_p$) for the major and (*S*,*R*$_p$) for the minor diastereomer. In addition, for complexes [$PdCl_2$(L)] (L = **1f**, **1i**), the (*R*,*R*$_p$) configuration was found for ligand **1f** and for the major diastereomer of ligand **1i**. These findings are in agreement with the view that the nucleophilic substitution of the dimethylamino group of intermediates **4** by a phosphino unit (step **4** → **5**, Scheme 1) takes place predominantly with overall retention of configuration at the stereogenic center.

Complexes [$PdCl_2$(L)] [L = (*R*,*R*$_p$)-**1d** and (*S*,*R*$_p$)-**1d**] both crystallize in the monoclinic space group $P2_1$ and contain one unit of chloroform per molecule. For each complex a hydrogen bond between $CHCl_3$ and Cl2 or Cl1 is observed. Despite their molecular similarity from a crystallographic point of view, complexes [$PdCl_2$((*R*,*R*$_p$)-**1d**)] and [$PdCl_2$((*S*,*R*$_p$)-**1d**)] are not isotypes. In the case of [$PdCl_2$((*R*,*R*$_p$)-**1d**)] the square-planar PdP_2Cl_2 unit is oriented almost parallel to (010), but the same plane is almost perpendicular to (010) in [$PdCl_2$((*S*,*R*$_p$)-**1d**)]. The unit cell parameters also differ significantly (Table 1).

(16) For the molecular structures of [$PdCl_2$((*R*,*R*$_p$)-**1d**)] and [$PtCl_2$(*R*,*R*$_p$)-**1d**)] in the solid state see: Maddox, A. F.; Rheingold, A. L.; Golen, J. A.; Kassel, W. S.; Nataro, C. *Inorg. Chim. Acta*, DOI: 10.1016/j.ica.2007.0.031.

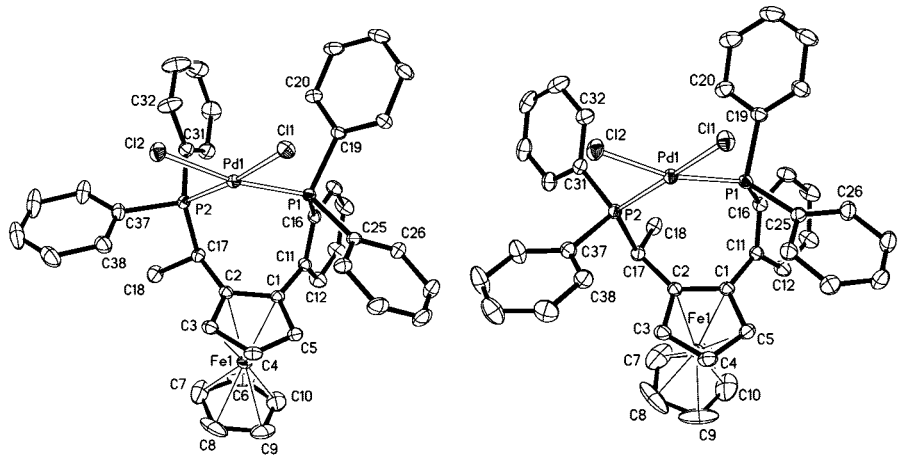

(R,R_p)-**1d** (S,R_p)-**1d**

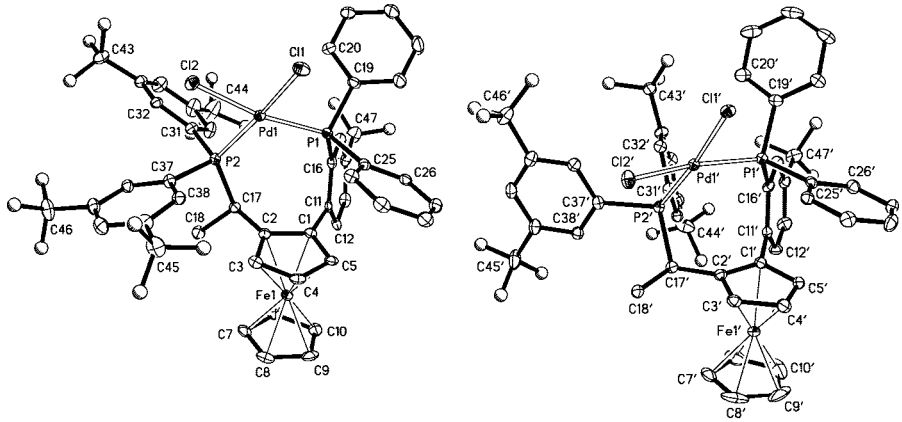

(R,R_p)-**1f**, molecule 1 (R,R_p)-**1f**, molecule 2

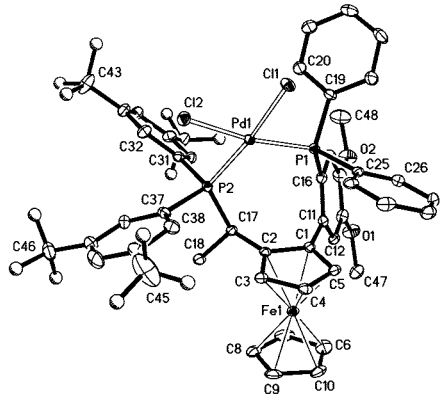

(R,R_p)-**1i**

Figure 1. Molecular structures of palladium dichloride complexes [$PdCl_2$(L)], L = (R,R_p)-**1d**, (S,R_p)-**1d**, (R,R_p)-**1f**, and (R,R_p)-**1i**. Compound [$PdCl_2$((R,R_p)-**1f**)] contains two independent complexes with singificantly different conformations, shown as molecule 1 and molecule 2. For clarity, F atoms are shown as spheres and not as ellipsoids. H-atoms and $CHCl_3$ solvent molecules are omitted.

Comparison of the two molecular structures shows that changing the configuration of ligand **1d** from (R,R_p) to (S,R_p) does not induce gross structural changes in the complex. However, significant differences are seen, especially in the orientation of the phenyl rings and the square-planar $PdCl_2$(P1,P2) unit (for a superposition of the two molecules see Figure 2, A). In both cases, bond lengths and bond angles of the ferrocene unit lie within the expected range. The cyclopentadienyl rings Cp (C1–C5) and Cp′ (C6–C10) are tilted with respect to each other by 6.4° and 5.8°, respectively (Table 2). The $PdCl_2$(P1,P2) units are located above the Cp ring, and only small deviations from the square-planar arrangement are observed. In the case of [$PdCl_2$((R,R_p)-**1d**)] the methyl group C18 is pointing toward proton H3 as well as to the unsubstituted Cp-ring (Cp′), while in [$PdCl_2$((S,R_p)-**1d**)] C18 is directed toward the backbone phenyl ring (C11–C16), an arrangement that leads to significant changes in bond angles C2–C1–C11 and C1–C2–C17 ([$PdCl_2$((R,R_p)-**1d**)]: 122.3° and 122.5°; [$PdCl_2$((S,R_p)-

Table 2. Geometrical Parameters of Complexes [$PdCl_2$(L)], L = (R,R_p)-1d, (S,R_p)-1d, (R,R_p)-1f, (R,R_p)-1i

	[$PdCl_2$((R,R_p)-**1d**)]	[$PdCl_2$((S,R_p)-**1d**)]	[$PdCl_2$((R,R_p)-**1f**)] mol 1	[$PdCl_2$((R,R_p)-**1f**)] mol 2	[$PdCl_2$((R,R_p)-**1i**)]
			Bond Lengths (Å)		
C1–C11	1.480(3)	1.479(2)	1.489(5)	1.494(5)	1.481(4)
C11–C12	1.386(3)	1.395(2)	1.391(5)	1.381(5)	1.397(4)
C11–C16	1.417(3)	1.408(2)	1.411(5)	1.416(5)	1.404(4)
C12–C13	1.374(4)	1.379(3)	1.397(6)	1.388(6)	1.388(4)
C13–C14	1.384(4)	1.385(3)	1.377(6)	1.392(6)	1.398(4)
C14–C15	1.388(4)	1.379(3)	1.390(6)	1.383(5)	1.383(4)
C15–C16	1.393(3)	1.399(2)	1.398(5)	1.392(5)	1.410(4)
C14–C47(CF_3)			1.508(6)	1.492(6)	
C13–O1					1.362(4)
C14–O2					1.365(4)
Pd1–P1	2.2796(5)	2.2856(6)	2.2841(10)	2.2773(10)	2.2964(7)
Pd1–P2	2.2693(6)	2.2573(7)	2.2665(10)	2.2514(10)	2.2508(7)
Pd1–Cl1	2.3535(6)	2.3493(7)	2.3294(10)	2.3387(10)	2.3377(7)
Pd1–Cl2	2.3535(6)	2.3370(7)	2.3513(10)	2.3402(10)	2.3381(7)
P1–C16	1.838(2)	1.840(2)	1.845(4)	1.842(4)	1.834(3)
P2–C17	1.868(2)	1.873(2)	1.860(4)	1.843(4)	1.851(3)
			Bond Angles (deg)		
Cl1–Pd–Cl2	87.78(3)	88.32(2)	88.55(4)	91.24(4)	86.85(3)
P1–Pd–P2	98.55(2)	104.22(2)	102.34(4)	97.83(4)	101.67(3)
C2–C1–C11	122.3(2)	129.1(2)	120.7(3)	131.4(3)	121.9(3)
C5–C1–C11	129.8(2)	123.5(2)	131.3(4)	121.1(4)	130.3(3)
C1–C2–C17	122.5(2)	128.7(2)	122.0(3)	128.3(3)	122.4(3)
C3–C2–C17	129.8(2)	124.2(2)	130.1(4)	124.2(3)	129.7(3)
C11–C16–P1	119.5(2)	120.6(1)	121.9(3)	121.5(3)	120.6(2)
C2–C17–P2	109.2(1)	109.4(1)	110.2(3)	110.8(3)	108.6(2)
			Tilt Angles (deg)		
Cp/Cp′	6.4(2)	5.8(2)	5.0(3)	4.8(3)	4.4(2)
Cp/P_2Pd	59.1(1)	78.9(1)	77.3(1)	60.5(1)	82.0(1)
Cp/P_2PdCl_2	63.0(1)	79.9(1)	77.1(1)	61.9(1)	73.5(1)
			Normal Distance of Atom from L.S. Plane through Cp Ring C1 to C5 (Å)		
C11/Cp	0.119(4)	0.026(3)	0.069(7)	0.231(7)	0.112(5)
C14/Cp	0.275(7)	–0.032(6)	0.078(12)	0.621(12)	0.253(9)
C17/Cp	0.113(4)	–0.009(3)	0.068(7)	0.176(7)	0.088(5)
C18/Cp	–0.913(5)	–0.565(4)	–1.021(8)	–0.333(9)	–1.051(6)
Pd1/Cp	3.583(2)	3.523(3)	3.652(5)	3.182(5)	3.602(3)
P1/Cp	2.907(3)	2.741(3)	2.901(5)	3.003(5)	2.890(4)
P2/Cp	1.876(4)	1.700(4)	1.778(7)	1.273(8)	1.761(5)
Cl1/Cp	5.494(2)	5.535(3)	5.663(4)	5.273(4)	5.648(2)
Cl2/Cp	4.648(4)	4.723(4)	4.757(8)	3.334(9)	4.656(5)
			Torsion Angles (deg)		
C1–C2–C17–C18	131.9(2)	23.8(3)	129.3(4)	172.7(4)	123.5(3)
C1–C2–C17–P2	–99.6(2)	–104.2(2)	–103.7(4)	–65.8(4)	–108.1(3)
C2–C1–C11–C16	74.5(3)	62.2(3)	75.3(5)	76.8(6)	73.2.(4)

1d)]: 129.1° and 128.7°). These changes in bond angle are associated with an increase in the tilt angle of the least-squares planes of Cp and the square-planar $PdCl_2$(P1,P2) unit from 63.0° to 79.9° (normal distances for Pd, Cl1, and Cl2 above Cp; [$PdCl_2$((R,R_p)-**1d**)]: 3.58, 5.49, 4.65 Å; [$PdCl_2$((S,R_p)-**1d**)]: 3.52, 5.54, 4.72 Å). In addition, conformational differences are observed for the Ph_2P phenyl rings, particularly for phenyl ring C31–C36.

Complexes [$PdCl_2$(L)] [L = (R,R_p)-**1f** and (R,R_p)-**1i**] crystallize in the orthorhombic space group $P2_12_12_1$ with two molecules in the asymmetric unit for complex [$PdCl_2$(**1f**)].

A superposition of these independent molecular structures of [$PdCl_2$(**1f**)] shows spectacular conformational differences (Figure 2, B). The main differences concern the phosphinoethyl side chain (for geometrical parameters see Table 2). In molecule 2 the side chain methyl group (C18) is positioned in close proximity to the least-squares plane of the substituted cyclopentadienyl ring (0.33 Å below Cp; torsional angle C18–C17–C2–C1: 172.7°). This places the phosphorus atom P2 at a distance of 1.27 Å above the Cp ring and one aryl ring, P2−Ar^1 (C31–C36), of the diarylphosphino unit in close proximity to the backbone aryl ring, Cp−Ar (C11–C16), with C31 located closest (normal distance of C31 to the least-squares plane of Cp−Ar defined by C11–C16: 3.12 Å). This interaction is associated with some significant molecular deformations. For example, the C1–C11 bond is strongly bent out of the Cp plane and this locates the Cp−Ar *ipso*- (C11) and *para*-carbon (C14) 0.23 and 0.61 Å, respectively, above that plane. In addition, bond angles C2–C1–C11 and C1–C2–C17 increase to 131.4° and 128.3°, respectively. Furthermore, the P2–C31 bond is tilted significantly out of the P2–Ar^1 plane, which places P2 at a position 0.22 Å away from the P2−Ar^1 plane.

In molecule 1 the diarylphosphino unit attached to the ethyl side chain adopts a totally different conformation. As compared to molecule 2, the whole phosphino ethyl unit is rotated clockwise about bond C2–C17 (C1–C2–C17–C18: 129.3°), which places C18 1.02 Å below and P2 1.78 Å above the Cp ring. In addition, the palladium atom is also moved further above Cp (molecule 2: 3.18 Å; molecule 1: 3.65 Å). Interestingly, in this conformation the bond angles C2–C1–C11 and C1–C2–C17 are decreased to 120.7° and 122.0°, respectively. In addition, the Cp−Ar ring (C11–C16) is bent toward the adjacent P−Ar^1 ring (C31–C36), which leads to C1 being 0.28 Å above the Cp−Ar plane. A very significant difference between molecules 1 and 2 is seen when both structures are viewed along the Pd1–P2 bond. In molecule 2 the Pd1–Cl2 bond dissects the bond

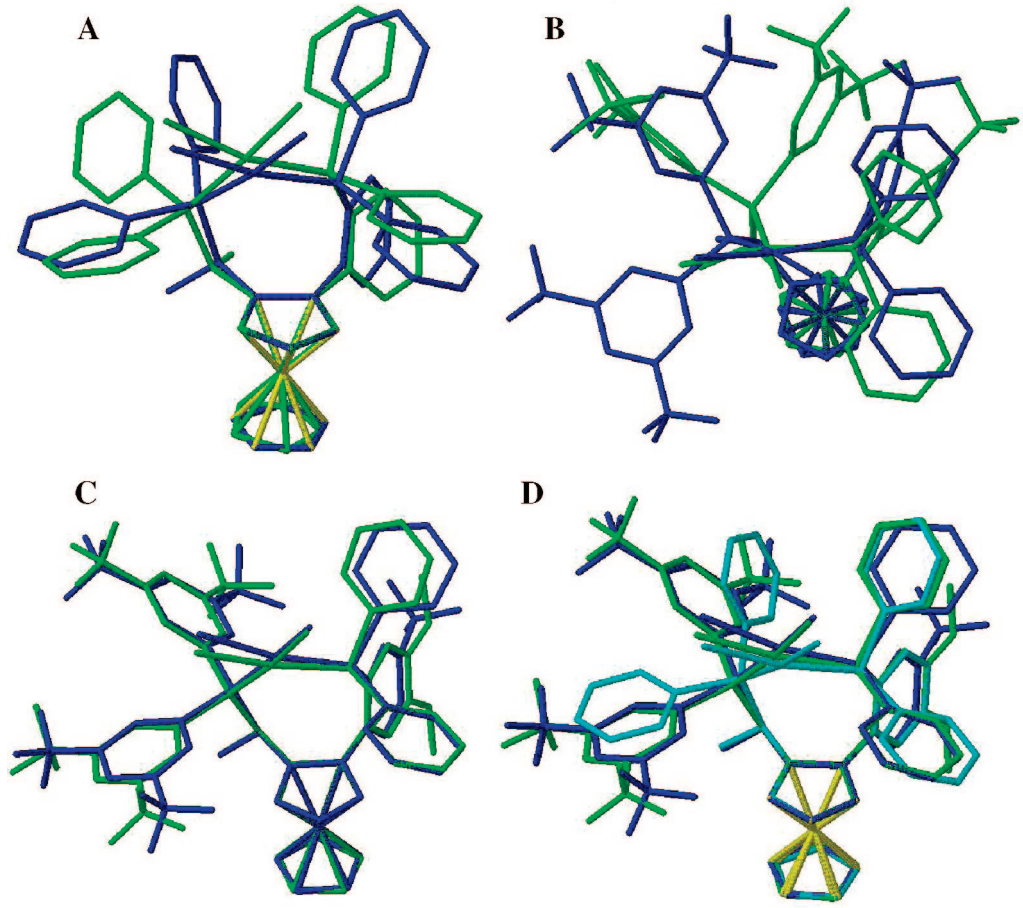

Figure 2. Superpositions of molecular structures of [$PdCl_2$((R,R_p)-**1d**)] (blue) and [$PdCl_2$((S,R_p)-**1d**)] (green) (A); [$PdCl_2$((R,R_p)-**1f**)], molecule 1 (blue) and [$PdCl_2$((R,R_p)-**1f**)], molecule 2 (green) (B); [$PdCl_2$((R,R_p)-**1f**)], molecule 1 (blue) and [$PdCl_2$((R,R_p)-**1i**)] (green) (C); [$PdCl_2$((R,R_p)-**1d**)] (light blue); [$PdCl_2$((R,R_p)-**1f**)], molecule 1 (dark blue) and [$PdCl_2$((R,R_p)-**1i**)] (green) (D).

angle C37–P2–C31, while in molecule 1 this bond is not positioned in between the P2-linked aryl rings but dissects the C17–P2–C37 bond angle.

Comparison of the two conformers of [$PdCl_2$(**1f**)] with that of [$PdCl_2$(**1i**)] shows that the overall structural features of molecule 1 in [$PdCl_2$(**1f**)] compare very well with those of complex [$PdCl_2$(**1i**)]. A superposition of these structures (Figure 2, C) shows that the main difference concerns the respective diphenylphosphino units.

In complex [$PdCl_2$(**1i**)] one methoxy methyl group C48 points toward one phosphorus-linked phenyl group, P1–Ph^1 (C19–C24), and this buttressing interaction clearly pushes P−Ph^1 in closer proximity to chloride Cl1. Otherwise, the conformational differences between [$PdCl_2$(**1i**)] and molecule 1 of [$PdCl_2$(**1f**)] are rather small.

In principle, the strong electronic effects associated with aryl substituents should be reflected in changes in the bond lengths of the respective aryl rings. A comparison of the trifluoromethyl- and methoxy-substituted aryl rings of complexes [$PdCl_2$(**1f**)] (molecule 1) and [$PdCl_2$(**1i**)] (C11–C16), however, shows that the lengths of the corresponding bonds differ only by a maximum of 0.021 Å (C13–C14 **1f**, molecule 1: 1.377 Å, **1i**: 1.398 Å, Table 2). Since similar differences in bond lengths are also observed for the conformers of [$PdCl_2$(**1f**)] (0.015 Å for bonds C13–C14; molecule 1: 1.377 Å; molecule 2: 1.392 Å, Figure 1), electronic effects of substituents cannot be considered the sole source of these changes.

In hydrogenation reactions Walphos (R,R_p)-**1d** has also been used as a reference ligand, and it was therefore of interest to compare the molecular structure of its dichloropalladium(II) complex [$PdCl_2$((R,R_p)-**1d**)] with those of complexes [$PdCl_2$((R,R_p)-**1f**)] and [$PdCl_2$((R,R_p)-**1i**)].

A superposition of all three structures is shown in Figure 2, D. Interestingly, the molecular structure of [$PdCl_2$(**1d**)] fits reasonably well with those of [$PdCl_2$(**1f**)] (molecule 1) and [$PdCl_2$(**1i**)]. Only the phenyl rings of the diphenylphosphino unit (Ph_2P2) linked to the ferrocenylethyl side chain adopt a slightly different conformation. These different arrangements are likely to be the result of the presence or absence of trifluoromethyl groups on these phosphorus-linked phenyl rings.

In summary, in the solid state the dichloropalladium complex of Walphos ligand **1f**, [$PdCl_2$(**1f**)], adopts two significantly different conformations, and these conformers differ mainly in the spatial arrangement of their diarylphosphino-substituted ethyl side chain. These marked structural differences indicate a rather high degree of conformational flexibility in such complexes. This conclusion is further supported by a recent finding by Nordlander et al.,[5] who showed that Walphos ligand **1c** can even coordinate to adjacent metals of a tetranuclear ruthenium cluster.

The structural differences observed for complexes of the backbone-substituted ligands **1f** and **1i** (one conformer of [$PdCl_2$(**1f**)] and [$PdCl_2$(**1i**)]) are rather small and are likely to be caused by both electronic and steric effects.

The molecular structures of complexes [$PdCl_2$(L)] [L = (R,R_p)-**1c**, (R,R_p)-**1d**, (R,R_p)-**1f**, and (R,R_p)-**1i**] in solution were determined by NMR spectroscopy, mainly by analyzing nuclear Overhauser interactions. The assignment of ^{1}H, ^{13}C, and ^{31}P

Table 3. Best Results Obtained in the Ruthenium- and Rhodium-Catalyzed Hydrogenation of Olefins and Ketones with Ligands 1a–1e

entry	substrate	ligand	catalyst precursor	$p(H_2)$ [bar]	T [°C]	time [h]	conv [%]	ee [%]
1	MAC	**1e**	$[Rh(NBD)_2]BF_4$	1	25	20.5	>99	95
2	MCA	**1c**	$[Rh(NBD)_2]BF_4$	5	25	20	>99	82
3	IPCA-D	**1c**	$[Rh(NBD)_2]BF_4$	50	25	8	>99	95
4	DMI	**1c**	$[Rh(NBD)_2]BF_4$	1	25	21	>99	91
5	ACA	**1c**	$[RuI_2(p\text{-cymene})]_2$	100	80	17	>99	97[a]
6	EOP	**1c**	$[RuI_2(p\text{-cymene})]_2$	100	80	16.5	>99	91
7	MPG	**1c**	$[Rh(NBD)_2]BF_4$	80	25	20.5	25	14

[a] *rac*:*meso* >99:1.

Chart 2. Substrates Used in Enantioselective Hydrogenation Reactions

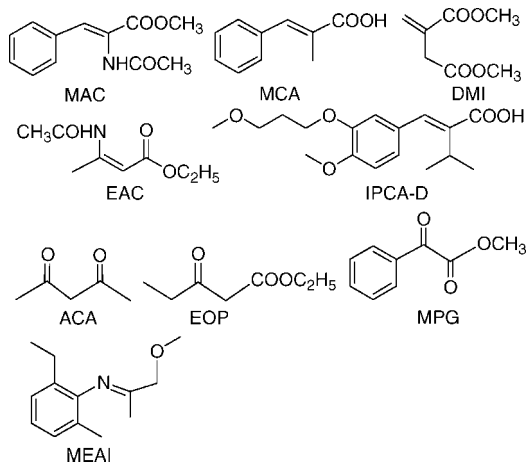

signals was made using standard one- and two-dimensional techniques. The ^{31}P spectra appear as one would expect; on complexation all phosphorus signals are shifted to lower field by about 40 ppm. However, the main structural information was obtained from proton and predominately from NOESY spectra. In all of these complexes, the observed NOEs are consistent with the solid-state structures. For complex $[PdCl_2((R,R_p)\text{-}\mathbf{1c})]$ a graphical representation of the main interactions that cause nuclear Overhauser enhancements is given in the Supporting Information.

Enantioselective Hydrogenations. As reported previously,[2] ligands **1a–1e** were screened in rhodium- and ruthenium-catalyzed hydrogenations of olefins and ketones. All catalysts were formed *in situ* using an appropriate Rh or Ru source and ligands of (R,R_p) configuration. The best results are listed in Table 3, and the substrates used are depicted in Chart 2. In most hydrogenation reactions, conversion was nearly quantitative, and for the majority of substrates it was possible to find ligands and reaction conditions that gave the product with very high to excellent enantioselectivity. In particular, ligand **1c** proved to be very valuable in rhodium-catalyzed hydrogenations of olefins as well as in ruthenium-catalyzed hydrogenations of ketones. The encouraging performance of this ligand in the hydrogenation of 2-methylcinnamic acid (MCA) (Table 3, entry 2) led essentially to the development of an industrial process for the enantioselective hydrogenation of a 2-isopropylcinnamic acid derivative (Chart 2, IPCA-D). Hydrogenation of this cinnamic acid derivative with a Rh catalyst generated *in situ* from $[Rh(NBD)_2]BF_4$ and ligand **1c** afforded, at 50 bar hydrogen pressure and ambient temperature, the corresponding saturated acid with 95% ee. This derivative is used as a chiral building block in the synthesis of the renin inhibitor aliskiren.

In general, in the hydrogenations tested, high product enantioselectivity was obtained only on using ligands bearing diarylphosphino units at both the stereogenic center and the backbone phenyl ring (**1c–1e**). In contrast, the use of ligands with a dialkylphosphino unit attached to the stereogenic center (**1a**, **1b**) in most cases resulted in products with rather poor enantioselectivity. As one would expect, ligand tuning was achieved by changing the steric and electronic properties of the phosphorus-bound aryl groups. In this respect, it is interesting to note that on using methyl (*Z*)-α-(acetamido)cinnamate (MAC) as the substrate, ligand **1e** [with an electron-donating phosphino group ($R = 3,5\text{-}(CH_3)_2\text{-}4\text{-}CH_3OC_6H_2$)] gave the best result, while ligand **1c** [with an electron-withdrawing phosphino group ($R = 3,5\text{-}(CF_3)_3C_6H_3$)] gave the best performance when 2-methylcinnamic acid (MCA) was the substrate (Table 3, entries 1 and 2).

The versatility of ligand **1c** (Table 3, entries 2–6) led us to question whether additional fine-tuning, especially of the electronic properties, could be achieved by attaching appropriate substituents to the backbone aryl ring at positions remote from the phosphino groups. As a result, ligands (R,R_p)-**1f–1i** with electron-withdrawing (**1f**: $R^1 = CF_3$, $R^2 = H$) or electron-donating (**1g**: $R^1 = CH_3$, $R^2 = H$; **1h**: $R^1 = OCH_3$, $R^2 = H$; **1i**: $R^1 = R^2 = OCH_3$) substituents were screened in rhodium-, ruthenium-, and iridium-catalyzed hydrogenation reactions of olefins, ketones, and one imine (for substrates tested see Chart 2 and Tables 4–6). The catalytic performance of these materials was compared with those of catalysts based on reference ligand **1c** and its bis-diphenylphosphosphino analogue **1d**. All catalysts were formed *in situ* using an appropriate Rh, Ru, or Ir source (see Tables 4–6), and for a given substrate, all reactions were carried out under identical reaction conditions.

In the rhodium-catalyzed hydrogenations of the alkenes methyl (*Z*)-α-(acetamido)cinnamate (MAC), (*Z*)-α-methylcinnamic acid (MCA), dimethyl itaconate (DMI), and ethyl (*Z*)-3-(acetamido)crotonate (EAC) (Table 4), replacement of the parent ligand **1c** by its analogues **1f–1i** only resulted in rather small changes in the catalytic performance. In almost all cases both conversion and enantioselectivity were hardly influenced. Only the use of DMI as the substrate and diphosphines **1g** and **1h** as the catalyst ligands gave rise to a significant loss of enantioselectivity (Table 4, entries 16 and 17). However, in general, the use of catalyst ligand **1d** led to much more pronounced changes in selectivity. On using **1d** as the catalyst ligand, two cases (MAC and DMI, Table 4, entries 2 and 14) gave significantly higher ee values and another two cases (MCA and EAC, Table 4, entries 8 and 20) gave significantly lower ee values than with ligands **1c** and **1f–1i**.

In the rhodium- and ruthenium-catalyzed hydrogenations of ketones (Table 5) the replacement of **1c** by diphosphines **1f–1i** as the catalyst ligands led to either an increase or a decrease in ee depending on the substrate used. The use of methyl phenylglyoxylate (MPG) as the substrate in conjunction with diphosphines **1f–1i** as the catalyst ligands (Table 5, entries 1 and 3–6) led to increases in enantioselectivity. In contrast, when the substrate was ethyl 3-oxopentanoate (EOP, entries 7 and 9–12), the ee values decreased in comparison to those obtained

Table 4. Rhodium-Catalyzed Hydrogenations of Alkenes with Ligands 1c, 1d, and 1f–1i

entry	substrate	ligand	catalyst precursor	$p(H_2)$ [bar]	T [°C]	time [h]	conv [%]	ee [%]
1	AC	**1c**	$[Rh(NBD)_2]BF_4$	1	25	1	50	60
2	MAC	**1d**	$[Rh(NBD)_2]BF_4$	1	25	1	100	89
3	MAC	**1f**	$[Rh(NBD)_2]BF_4$	1	25	1	34	56
4	MAC	**1g**	$[Rh(NBD)_2]BF_4$	1	25	1	47	63
5	MAC	**1h**	$[Rh(NBD)_2]BF_4$	1	25	1	49	67
6	MAC	**1i**	$[Rh(NBD)_2]BF_4$	1	25	1	47	60
7	MCA	**1c**	$[Rh(NBD)_2]BF_4$	5	25	16	100	87
8	MCA	**1d**	$[Rh(NBD)_2]BF_4$	5	25	16	100	70
9	MCA	**1f**	$[Rh(NBD)_2]BF_4$	5	25	16	100	85
10	MCA	**1g**	$[Rh(NBD)_2]BF_4$	5	25	16	100	86
11	MCA	**1h**	$[Rh(NBD)_2]BF_4$	5	25	16	100	85
12	MCA	**1i**	$[Rh(NBD)_2]BF_4$	5	25	16	100	81
13	DMI	**1c**	$[Rh(NBD)_2]BF_4$	1	25	1	50	41
14	DMI	**1d**	$[Rh(NBD)_2]BF_4$	1	25	1	32	83
15	DMI	**1f**	$[Rh(NBD)_2]BF_4$	1	25	1	11	42
16	DMI	**1g**	$[Rh(NBD)_2]BF_4$	1	25	1	100	rac
17	DMI	**1h**	$[Rh(NBD)_2]BF_4$	1	25	1	72	8
18	DMI	**1i**	$[Rh(NBD)_2]BF_4$	1	25	1	28	32
19	EAC	**1c**	$[Rh(NBD)_2]BF_4$	1	25	16	14	35
20	EAC	**1d**	$[Rh(NBD)_2]BF_4$	1	25	16	30	14
21	EAC	**1f**	$[Rh(NBD)_2]BF_4$	1	25	16	3	36
22	EAC	**1g**	$[Rh(NBD)_2]BF_4$	1	25	16	8	32
23	EAC	**1h**	$[Rh(NBD)_2]BF_4$	1	25	16	7	25
24	EAC	**1i**	$[Rh(NBD)_2]BF_4$	1	25	16	7	25

Table 5. Ruthenium- and Rhodium-Catalyzed Hydrogenations of Ketones with Ligands 1c, 1d, and 1f–1i

entry	substrate	ligand	catalyst precursor	$p(H_2)$ [bar]	T [°C]	time [h]	conv [%]	ee [%]
1	MPG	**1c**	$[Rh(NBD)Cl]_2$	80	25	20.5	25	14
2	MPG	**1d**	$[Rh(NBD)Cl]_2$	80	25	20.5	26	41
3	MPG	**1f**	$[Rh(NBD)Cl]_2$	80	25	20.5	3	20
4	MPG	**1g**	$[Rh(NBD)Cl]_2$	80	25	20.5	8	31
5	MPG	**1h**	$[Rh(NBD)Cl]_2$	80	25	20.5	12	39
6	MPG	**1i**	$[Rh(NBD)Cl]_2$	80	25	20.5	14	34
7	EOP	**1c**	$[RuI_2(p\text{-cymene})]_2$	80	80	16	96	91.5
8	EOP	**1d**	$[RuI_2(p\text{-cymene})]_2$	80	80	16	100	77
9	EOP	**1f**	$[RuI_2(p\text{-cymene})]_2$	80	80	16	100	78
10	EOP	**1g**	$[RuI_2(p\text{-cymene})]_2$	80	80	16	100	90
11	EOP	**1h**	$[RuI_2(p\text{-cymene})]_2$	80	80	16	100	88
12	EOP	**1i**	$[RuI_2(p\text{-cymene})]_2$	80	80	16	100	83.5

Table 6. Iridium-Catalyzed Hydrogenations of (*E*)-2-Ethyl-*N*-(2-methoxy-1-methylethylidene)-6-methylaniline, MEAI, with Ligands 1c, 1d, and 1f–1i

entry	substrate	ligand	catalyst precursor	$p(H_2)$ [bar]	T [°C]	time [h]	conv [%]	ee [%]
1	MEAI	**1c**	$[Ir(COD)Cl]_2$	80	25	16	100	33
2	MEAI	**1d**	$[Ir(COD)Cl]_2$	80	25	16	80	14
3	MEAI	**1f**	$[Ir(COD)Cl]_2$	80	25	16	94	7
4	MEAI	**1g**	$[Ir(COD)Cl]_2$	80	25	16	87	43
5	MEAI	**1h**	$[Ir(COD)Cl]_2$	80	25	16	91	30
6	MEAI	**1i**	$[Ir(COD)Cl]_2$	80	25	16	91	36

with **1c**. In all of these cases the maximum changes in ee values are comparable to those obtained with reference ligand **1d** (Table 5, entries 2/5 and 8/9).

An interesting trend in catalyst performance was observed in the iridium-catalyzed hydrogenation of (*E*)-2-ethyl-*N*-(2-methoxy-1-methylethylidene)-6-methylaniline (MEAI). Replacement of the reference catalyst ligand **1c** by the trifluoromethyl-substituted ligand **1f** led to a drop in enantioselectivity (Table 6, entries 1 and 3), while use of the methyl- or methoxy-substituted ligands **1g** and **1i** resulted in slightly higher ee values (Table 6, entries 4 and 6).

Overall, substitution of Walphos ligand **1c** at remote positions 4 (or 4 and 5) of the ferrocene-linked phenyl ring with electron-withdrawing or electron-donating substituents only allows limited tuning of the performance of rhodium-, ruthenium-, and iridium-based hydrogenation catalysts. In hydrogenation reactions involving alkenes the effects of such changes on conversion and enantioselectivity of the product are rather small, and in the hydrogenation of two ketones and one imine increases of up to 25% ee (MPG) could be obtained, albeit with a rather low level of enantioselectivity.

Concluding Remarks

The use of Walphos-type ligands, especially those having diarylphosphino units attached to the phenyl-ferrocenylethyl scaffold, in ruthenium- and rhodium-catalyzed asymmetric hydrogenations of olefins and ketones enables enantioselectivities of up to 95% and 97% ee, respectively, to be obtained. Most interestingly, one Walphos-type ligand (**1c**) performed very well in the rhodium-catalyzed hydrogenation of 2-alkyl-substituted cinnamic acids, and this led to the development of a large-scale process for the asymmetric hydrogenation of a 2-isopropylcinnamic acid derivative. The product obtained in this process (a 2-isopropyl-3-arylpropionic acid) is used as a chiral building block in the synthesis of renin inhibitor aliskiren.

In an effort to obtain optimal catalyst performance, ligands were tuned mainly by varying the steric and electronic properties of the phosphorus-bound aryl rings. In addition, substitution of Walphos at remote positions 4 (or 4 and 5) of the ferrocene-linked phenyl ring with electron-withdrawing or electron-donating substituents allowed further tuning of the performance of the hydrogenation catalysts, but only to a very limited degree.

The molecular stuctures of dichloropalladium(II) complexes of four Walphos-type ligands were studied by X-ray diffraction. In each case the ligand was found to be coordinated to palladium in a bidentate fashion. Surprisingly, in the solid state the dichloropalladium complex of ligand **1f**, [$PdCl_2$(**1f**)], adopts two significantly different conformations. These conformers differ markedly in the spatial arrangement of their diarylphosphino-substituted ethyl side chain, indicating a rather high degree of conformational flexibility in such complexes. On the other hand, replacement of the trifluoro-substituted ligand **1f** by the methoxy-substituted ligand **1i** hardly changed the overall complex geometry. The differences between the molecular structure of one conformer of complex [$PdCl_2$(**1f**)] and that of [$PdCl_2$(**1i**)] were found to be rather small. As determined by NMR spectroscopy, in all of the complexes investigated the molecular structure in solution corresponded to that in the solid state.

Experimental Section

Standard Procedure for Hydrogenation Reactions. The substrate (2.53 mmol) and the catalyst (formed *in situ*, see below) were dissolved separately in the appropriate solvent (5 mL) under argon (total volume: 10 mL). The catalyst solution was stirred for 15 min. Both the catalyst and the substrate solutions were transferred through a steel capillary into a 180 mL thermostatted glass reactor or a 50 mL stainless steel autoclave. The inert gas was then replaced by hydrogen (three cycles) and the pressure was set. After completion of the reaction (total reaction times 1–21 h, see Tables 3–6) the conversion was determined by gas chromatography, and the product was recovered quantitatively after filtering the reaction solution through a plug of silica. The enantiomeric purity of the product was determined either by gas chromatography or by HPLC.

The following reaction conditions and methods for ee determination were applied:

MAC: 2.53 mmol (0.25 mol/L) of MAC; $[Rh(NBD)_2][BF_4]$ + 1.05 equiv of ligand; s/c = 200; solvent: MeOH (10 mL); $p(H_2)$: 1 bar; 25 °C; reaction time: 1 h; ee: GC, Chirasil-L-Val, 170 °C, isotherm.

MCA: 2.53 mmol (0.25 mol/L) of MCA; $[Rh(NBD)_2][BF_4]$ + 1.05 equiv of ligand; s/c = 200; solvent: MeOH (10 mL); $p(H_2)$: 5 bar; 25 °C; reaction time: 16 h; ee: as methyl ester; HPLC; Chiralcel OB, hexane/iPrOH: 98:2, 0.1 mL/min.

DMI: 2.53 mmol (0.25 mol/L) of DMI; $[Rh(NBD)_2][BF_4]$ + 1.05 equiv of ligand; s/c = 200; solvent: MeOH (10 mL); $p(H_2)$: 1 bar; 25 °C; reaction time: 1 h; ee: GC, Lipodex E, 80 °C, isotherm.

EAC: 2.53 mmol (0.25 mol/L) of EAC; $[Rh(NBD)_2][BF_4]$ + 1.05 equiv of ligand; s/c = 200; solvent: EtOH (9.5 mL); additive: 2,2,2-CF_3CH_2OH (0.5 mL); $p(H_2)$: 1 bar; 25 °C; reaction time: 16 h; ee: GC, Betadex 110 (Supelco), 120 °C isotherm.

ACA: 2.53 mmol (0.25 mol/L) of ACA; $[RuI_2(p\text{-cymene})]_2$ + 2.2 equiv of ligand; s/c = 1000; solvent: MeOH (10 mL); additive: 1 N HCl (aq): 120 μL; $p(H_2)$: 100 bar; 80 °C; reaction time: 17 h; ee: as bis(trifluoroacetate); GC, Lipodex E, 80 °C, isotherm.

MPG: 2.53 mmol (0.25 mol/L) of MPG; $[Rh(NBD)Cl]_2$ + 2.1 equiv of ligand; s/c = 200; solvent: toluene (10 mL); $p(H_2)$: 80 bar; 25 °C; reaction time: 20.5 h; ee: HPLC; Chiralcel OJ, hexane/*i*PrOH: 90:10, 1.0 mL/min.

EOP: 2.53 mmol (0.25 mol/L) of EOP; $[RuI_2(p\text{-cymene})]_2$ + 2.1 equiv of ligand (no pretreatment); s/c = 200; solvent: EtOH (10 mL); additive: 1 N HCl (aq): 60 μL; $p(H_2)$: 80 bar; 80 °C; reaction time: 16 h; ee: as trifluoroacetate derivative; GC, Lipodex E, 80 °C, isotherm.

MEAI: 2.53 mmol (0.25 mol/L) of MEAI; $[Ir(COD)Cl]_2$; + 2.1 equiv of ligand; s/c = 100; solvent: toluene (10 mL); additives: tetrabutylammonium iodide (2 equiv/Ir), CF_3COOH (30 μL); $p(H_2)$: 80 bar; 25 °C; reaction time: 16 h; ee: as trifluoroacetate derivative, GC, Lipodex E, 80 °C, isotherm.

IPCA-D: 78 mmol of IPCA-D in 140 mL of MeOH; $[Rh(NBD)_2][BF_4]$ + 1.05 equiv of ligand in 20 mL of MeOH; s/c = 5000; $p(H_2)$: 50 bar; 25 °C; reaction time: 8 h; ee: as methyl ester; HPLC; Chiralcel OB, MeCN/H_2O: 3:7. For further details on the hydrogenation of IPCA-D see ref 3.

X-ray Structure Determination. Crystals of [$PdCl_2$((R,R_p)-**1d**)], [$PdCl_2$((S,R_p)-**1d**)], [$PdCl_2$((R,R_p)-**1f**)], and [$PdCl_2$((R,R_p)-**1i**)] in the form of $CHCl_3$ solvates with 1, 1, 0.5, and 3 $CHCl_3$ per metal complex, respectively, were obtained by slow diffusion of Et_2O into solutions of the corresponding complex in $CHCl_3$. Crystal data and experimental details are given in Table 1. X-ray data were collected on Bruker Smart CCD area detector diffractometers using graphite-monochromated Mo Kα radiation (λ = 0.71073 Å) and φ- and ω-scan frames covering complete spheres of the reciprocal space. Corrections for absorption, $\lambda/2$ effects, and crystal decay were applied.[17] The structures were solved by direct methods using the program SHELXS97.[18] Structure refinement on F^2 was carried out with the program SHELXL97. All non-hydrogen atoms were refined anisotropically. Hydrogen atoms were inserted in idealized positions and were refined riding with the atoms to which they were bonded. Modest orientation disorder of the $CHCl_3$ solvent molecules for [$PdCl_2$((R,R_p)-**1d**)] and [$PdCl_2$((R,R_p)-**1i**)] was taken into account. The $CHCl_3$ solvates of [$PdCl_2$((R,R_p)-**1d**)], [$PdCl_2$((S,R_p)-**1d**)], and [$PdCl_2$((R,R_p)-**1f**)] are stable under ambient conditions and do not lose solvent. All four solvates are stabilized by C–H---Cl hydrogen bonds between $CHCl_3$ and the Pd-bound Cl atoms. Selected geometric data are presented in Table 2. Further details are given in the Supporting Information.

Acknowledgment. This work was kindly supported by Solvias AG, Basel.

Supporting Information Available: Details on the synthesis of all ligands and complexes, crystal data for the hydroiodide salt of intermediate **3A**, as well as complete crystallographic data and technical details in CIF format for compounds [$PdCl_2$((R,R_p)-**1d**)], [$PdCl_2$((S,R_p)-**1d**)], [$PdCl_2$((R,R_p)-**1f**)], [$PdCl_2$((R,R_p)-**1i**)], and [**3A**(HI)]. This material is available free of charge via the Internet at http://pubs.acs.org.

OM701103D

(17) Bruker programs: *SMART*, version 5.629; *SAINT*, version 6.45; *SADABS*, version 2.10; *XPREP*, version 6.1; *SHELXTL*, version 6.14; Bruker AXS Inc.: Madison, WI, 2003.

(18) Sheldrick, G. M. *SHELX97*, Program System for Crystal Structure Determination; University of Göttingen: Göttingen, Germany, 1997.